An Elastic Analysis of *Listeria monocytogenes* Propulsion

Fabien Gerbal,* Paul Chaikin,† Yitzhak Rabin,‡ and Jacques Prost*
*UMR 168 "Physico-chimie," CNRS/Institut Curie, Section de Recherche, 75248 Paris, France; †Department of Physics, Princeton University, Princeton, New Jersey 08544 USA; and ‡Department of Physics, Bar-Ilan University, Ramat-Gan 52900, Israel

ABSTRACT The bacterium *Listeria monocytogenes* uses the energy of the actin polymerization to propel itself through infected tissues. In steady state, it continuously adds new polymerized filaments to its surface, pushing on its tail, which is made from previously cross-linked actin filaments. In this paper we introduce an elastic model to describe how the addition of actin filaments to the tail results in the propulsive force on the bacterium. Filament growth on the bacterial surface produces stresses that are relieved at the back of the bacterium as it moves forward. The model leads to a natural competition between growth from the sides and growth from the back of the bacterium, with different velocities and strengths for each. This competition can lead to the periodic motion observed in a *Listeria* mutant.

INTRODUCTION

Many biological movements are based on the dynamics of the actin network in cells; this is the case, for instance, for the process of the lamellipodia extension in crawling cells (Wang, 1985) or the motion of the neural cone during dendrite growth (Bray et al., 1991). To produce the forces required for the motion, actin is often associated with myosin, as in muscles or in the cell contractile ring (Bray, 1992). However, the presence of motor proteins like myosins is not necessary to produce a motile force; this issue has been discussed for ameboid motion (Mitchison and Cramer, 1996) and has been demonstrated several times in the case of the bacterium *Listeria monocytogenes*, for which motor proteins associated with its actin tail have been sought but not found (Mounier et al., 1990; Marchand et al., 1995; Southwick and Purich, 1998; Loisel et al., 1999). It is therefore widely accepted that the process of actin polymerization itself is sufficient to induce cell movements. Physical models of actin-based motility have been suggested in the case of ameboid motion (Evans, 1993; Alt and Dembo, 1999) and by Mogilner and Oster (1996), who have proposed a generic Brownian ratchet mechanism that also describes the growth of microtubules (Mogilner and Oster, 1999).

In this paper, we will focus on the case of *Listeria*, a system for which a lot of experimental data are available. The characteristic numbers for *Listeria* motion and the notations that will be used in the following are listed in Table 1. To move within cell cytoplasm and spread from cell to cell through the cytoplasmic membranes, *L. monocytogenes* induces the assembly of a tail (Fig. 1), which is an actin gel made of cross-linked filaments and which forms a tubular structure (Tilney and Portnoy, 1989). The actin is recruited from the pool of the infected cell. The tail is used as an anchor in the cytoplasm, so that as new polymerized actin is added between the bacterium surface and the older polymerized gel, the organism is propelled forward (Theriot et al., 1992). This type of motion has recently been shown to be more general than initially thought: besides the Gram-positive *L. monocytogenes* and the Gram-negative *Shigella flexneri* (Clerc and Sansonetti, 1987), the intracellular movements of the vaccinia virus (Cudmore et al., 1995) and even of some vesicles (Merrifield et al., 1999) are based on the formation of an actin tail. In *Listeria*, the presence of a single transmembrane protein, ActA, has been shown to be required and sufficient to trigger actin polymerization and thus to induce the motion (Kocks et al., 1992; Smith et al., 1995). Immunolabeling experiments have shown that ActA is present everywhere around the moving *Listeria*, except at the front pole (defined by the direction of motion) and that ActA colocalizes with the production of actin filaments (Kocks et al., 1993). All of the other proteins like actin, the cross-linkers such as α-actinin (Dabiri et al., 1990) and other proteins required for the actin polymerization (like Arp2/3; Welch et al., 1997), are provided by the infected medium. Recently the motility of *Listeria* has been observed in a medium reconstituted from pure proteins (Loisel et al., 1999). Although several biochemical scenarios have been suggested (Southwick and Purich, 1998; Cossart and Kocks, 1994), the enzymatic reactions responsible for the local shift of the actin monomeric/polymeric equilibrium around the bacterium have not been completely elucidated. Some progress has been made in determining the kinetics of nucleation and of the growth of the actin filaments (Welch et al., 1998), but the time constants for the release from the surface and the cross-linking of the filaments are not yet known.

In a recent paper (Gerbal et al., 2000) we presented results on some of the elastic properties of the actin filament tail. We found that the tail is firmly attached to the bacterium; applying a force in the picoNewton range between the bacterium and its tail for several minutes failed to pull the

Received for publication 14 February 2000 and in final form 9 August 2000.

Address reprint requests to Dr. Fabien Gerbal, UMR 168 "Physico-chimie," CNRS/Institut Curie, Section de Recherche, 11 rue Pierre et Marie Curie, 75231 Paris Cedex 05, France. Tel.: 33-(0)1-55-86-28-16; Fax: 33-(0)1-40-51-06-36; E-mail: gerbal@curie.fr.

0006-3495/00/11/2259/17 $2.00

TABLE 1 Main parameters describing the motion of *Listeria monocytogenes* used in the text

Parameters	Variable name	Typical value observed
Listeria length	L	1.5 μm
Listeria radius	r_b	0.5 μm
Tail length	Not used (∞)	5–200 μm
Tail external radius (3D model)	$r_b(1 + \delta)$	0.5–1 μm
Gel thickness above the bacterium	β	$0.5 < \beta < 2$
Gel thickness above the bacterium at the rear	$\alpha = (r_m - r_b)/r_b$	$0.5 < \alpha < 2$
Bacterium cross section	$S_b = \pi r_b^2$	1 μm^2
Tail cross section, 1D model	S_{t_1}	1 μm^2
Tail cross section, 3D model	$S_{t_2} = \pi r_b^2(1 + \delta)^2$	1 μm^2
Actin tail Young's modulus	Y	10^3 to 10^4 Pa
Listeria speed	v	0.1–0.2 $\mu m \cdot s^{-1}$ (no external force)
Growth speed of the internal (external) gel	$v_{p_{1(2)}}$	Unknown
Number of filaments around the bacterium	Not used	100–1000
Friction coefficient between the gel and the bacterium	γ	$10^{-4} < \gamma < 1$ Pa · m · s (see text)
Force exerted by the internal gel on the bacterium	$F_1 = F_{mot_1}$	See text
Force exerted by the external gel on the bacterium	$F_2 = F_{mot_2} + F_{fric}$	See text

bacterium from its tail. We have also shown in this paper that the tail behaves like a genuine gel: optical tweezers were used to apply stresses, and we found that the tail's response is elastic. This finding is consistent with the presence of actin-binding cross-linkers (Dabiri et al., 1990). The strong attachment of the bacterium to the tail puts limits on the thermal ratchet model of propulsion, where actin filaments simply push on the bacterium to which they are not

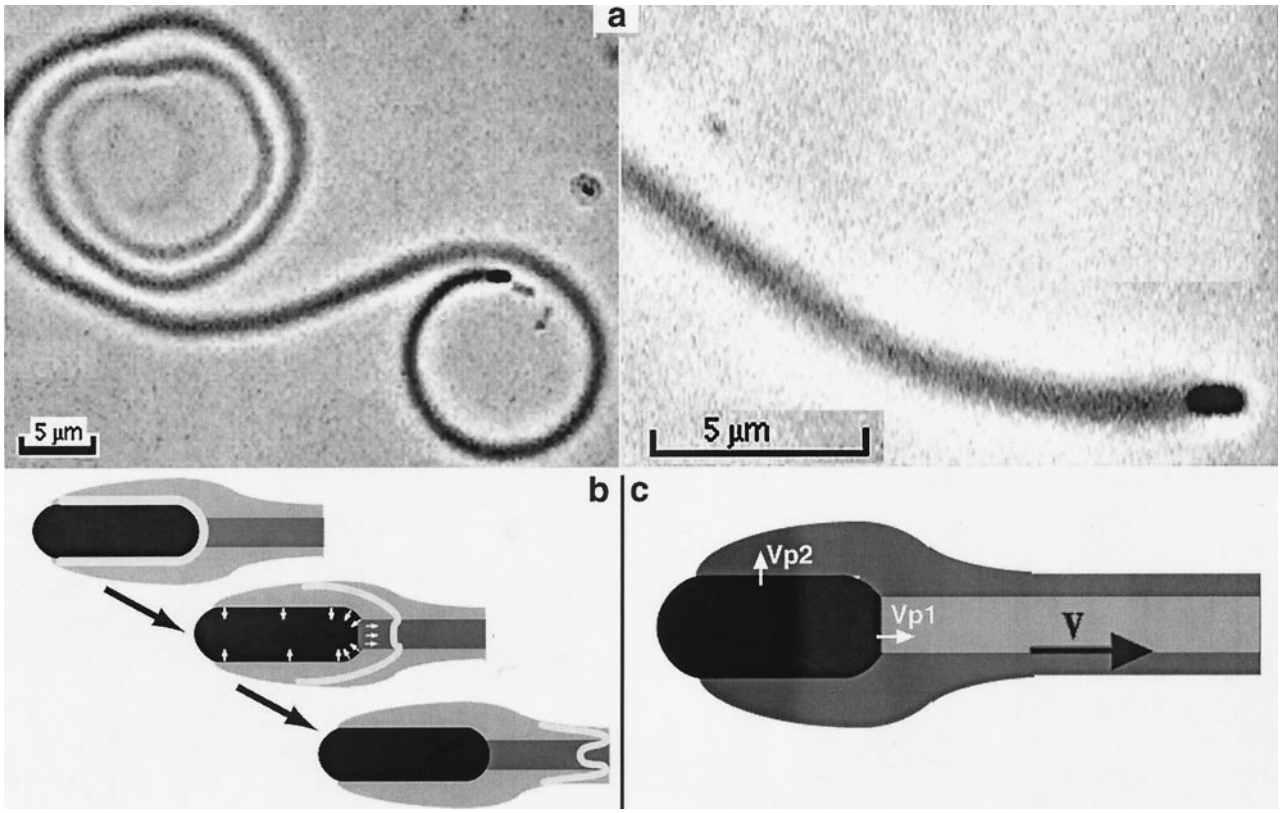

FIGURE 1 (*a*) Observation of *Listeria* moving in platelet extract, observed by phase-contrast microscopy. The bacteria move at ~8 $\mu m \cdot min^{-1}$. The tail can be more than 100 μm long when the depolymerization is slow enough. Bars = 5 μm. (*b*) Elastic model of the propulsion of the bacterium: the new filaments are polymerized at the bacterium surface and expand the older layers, inducing a stress in the actin gel, which is viewed as a continuous medium. The motion of the bacterium is due to the relaxation of the strain in the tail. (*c*) Heuristic model: the system is simplified in a two-gel model; the internal gel is produced on the back hemisphere at the polymerization speed v_{p_1}, and the external gel is produced on the cylindrical surface at v_{p_2}. The gel is a single structure that moves away from the bacterium at the homogeneous speed v.

attached (Mogilner and Oster, 1996). The observed attachment suggests that the force between the bacterium and its tail results from the distortions of a continuous elastic medium (a gel) anchored to and growing from the bacterium surface. The bending modulus K of the tail was measured and found to be on the order of 100–1000 Pa (μm)^4 (persistence length ~0.1 m), suggesting a Young's modulus $Y = [K/\pi(r_b^4/4)] = 10^3$ to 10^4 Pa for the actin gel.

We are therefore led to a mesoscopic description of the *Listeria* motility at a length scale larger than that of individual proteins. Although there has been a great effort expended in the discovery of many of the microscopic aspects of the polymerization process and the specific proteins involved, the propulsion mechanism that arises from the growth and cross-linking of the filaments is important and interesting in its own right. It is also necessary for the basic understanding of the mechanisms that control the speed of the bacterium, the maximum force it can overcome, and the effect of the obstacles and forces it encounters during its motion. In this paper we describe the gel as a continuous medium that can be treated in the framework of the linear theory of elasticity. We propose that the addition of new actin filaments induces elastic deformations in the gel: the buildup of a new polymerized layer at the bacterium surface compresses the previously formed layers. Thus, the free energy produced by actin polymerization is not directly used for the propulsion but is rather first stored as elastic energy (Fig. 1 *b*). The problem is significantly complicated by the actual geometry of the bacterial surface, which produces the filaments. Consider the cylindrical surface of the bacterium. If the filaments were not cross-linked, they would grow radially outward, hindering rather than aiding the propulsion. Because the filaments are cross-linked, the outward growth can only be accomplished by an extension of tangential cross-links as they are forced to a larger radius. This costs a large elastic energy ($\propto R_{gel}^3$), produces a large stress on the cell surface, and eventually leads to a cessation of growth, as has been demonstrated experimentally on beads (Noireaux et al., 2000; Gerbal et al., 1999). The shape of the gel and, therefore, the motion of the bacterium depend on the way the gel adopts the lowest energy conformation. In fact, for most geometries there are no steady-state solutions that allow continued growth without a steady increase in elastic energy. The only geometry that allows continued growth for a cross-linked system corresponds to one-dimensional growth, i.e., to a long region of constant cross section, such as the *Listeria* tail.

For the sake of simplicity, we will discuss this problem, using a two-gel model (Fig. 1 *c*), in which the gel is artificially divided into two parts: the internal gel, produced from the back part of the bacterium (gel number 1: *light gray* in the figure), and the external gel, produced on the cylindrical surface (gel number 2: *dark gray*). First, we will consider the simplest case of a bacterium producing only the internal gel. Then we will consider the case of a bacterium pushed only by the external gel. Finally, we will present the complete model in which a bacterium is pushed by both gels. Despite its simplicity, this two-gel model provides important insights into the distortion of a gel produced in quasi-3D geometry before being constrained to a 1D geometry. Furthermore, the two-gel model allows us to understand the behavior of a *Listeria* mutant ($ActA_{\Delta 21-97}$) obtained by Lasa et al. (1997): the speed of this mutant oscillates periodically between a very slow and a fast phase. In the last part of the paper we extend the steady-state equations of the elastic model to describe time-dependent processes and show that the resulting model can also explain the mechanism of these oscillations.

STEADY-STATE MOTION

One-dimensional model

The easiest mechanism of propulsion to imagine would occur if the actin were simply polymerized at a constant polymerization speed v_{p_1} (index 1 is used for the description of the internal gel, and index 2 will be used for the external gel produced at the cylindrical surface) from a flat region at the end of the bacterium (Fig. 2). We will describe *Listeria* as a cylinder with a circular cross section of area $S_b = \pi r_b^2$ and assume in the 1D model that the gel is produced only at the back of the bacterium. The elastic deformations of the gel relevant for propulsion occur on distances much smaller (typically the size of the bacterium) compared to the length scale on which the depolymerization of the actin in the tail becomes relevant (<10 μm). The tail is therefore modeled as an infinitely long tube of cross-sectional area S_{t_1}, made of homogeneous elastic material. It is characterized by a compressional modulus Y and an axial elastic strain ϵ_1. In the reference frame of the bacterium, the tail moves away at a speed v. This is the parameter that we want to determine as a function of F_{ext}, the external force applied on the bacte-

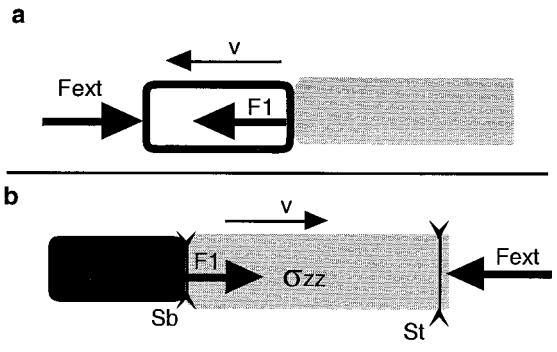

FIGURE 2 Schematic representation of the forces applied on the bacterium in the one-dimensional model. (*a*) The tail exerts the force $F_1 = F_{mot_1}$ on the bacterium, which moves against the external force F_{ext}. (*b*) We solve the problem in the reference frame of the bacterium; the tail moves away at the speed v. F_{ext} is also exerted on any section of the tail of surface S_{t_1}, inducing an axial stress σ_{zz}.

rium. We will neglect viscous forces due to the friction against the outer medium; for cytoplasm viscosity on the order of 10^{-2} Pa · s, this force is ~10 fN, which is negligible in comparison with the forces involved in the propulsion of *Listeria.*

The forces exerted on the bacterium must balance each other, so we have $F_{\mathrm{mot_l}} = -F_{\mathrm{ext}}$, where $F_{\mathrm{mot_l}}$ is the force from the tail on the bacterium. From Newton's second law (action = reaction), F_{ext} is also exerted on any cross section of the tail and must be balanced by the elastic stresses σ_{ij} in the tail that must fulfill the condition $\nabla_i \sigma_{ij} = 0$ (Landau and Lifchitz, 1967). Consistent with the neglect of viscous frictional forces, both the radial and the shear components of the stress must vanish on the cylindrical surface of the tail. The axial component of the stress is therefore

$$\sigma_l \triangleq \sigma_{zz} = -\frac{F_{\mathrm{ext}}}{S_{t_l}} \tag{1}$$

Linear elasticity relates this stress to the longitudinal strain in the tail:

$$\varepsilon_l \triangleq \varepsilon_{zz} = \frac{\sigma_l}{Y} \tag{2}$$

For the sake of simplicity, we assume that the tail is incompressible, i.e., that the volume of a material element is conserved under deformation (Poisson ratio = 1/2). This is consistent with elasticity measurements which showed that the Poisson ratio of a fibroblast actin cortex is ~0.4 (Sackmann, personal communication). Using volume conservation relates the elongation of a cylindrical element of nondeformed material (of length Δz and cross-sectional area S_b) with that of a similar element in the tail (of length $\Delta z'$): $\Delta z S_b = \Delta z' S_{t_l}$, and we obtain

$$\epsilon_l = \frac{S_b}{S_{t_l}} - 1 \tag{3}$$

Another requirement of continuous production of actin fibers is that they must go somewhere. Polymerization takes place at the bacterium surface and actin depolymerizes along the tail, because the infected cytoplasm cell sets a new equilibrium in favor of the nonpolymerized form of actin. Between these two regions we can account for the quantity of F-actin filaments by conservation of flow. The rate at which filaments are produced on the entire surface of the bacterium is equal to the total flux through any cross section of the tail (before depolymerization becomes important):

$$v_{p_l} S_b = v S_{t_l} \tag{4}$$

We can now write the force-velocity equation:

$$\frac{v}{v_{p_l}} = \frac{1}{1 + F_{\mathrm{ext}}/YS_b} \tag{5}$$

The plot of this equation is shown in Fig. 3. The characteristic scale of elastic force in our model is therefore given by $YS_b = 1$ nN, which is several orders of magnitude greater than the typical force that is encountered by the bacterium when it moves through an infected medium. For instance, the force required to deform a membrane is on the order of 50 pN (Evans and Yeung, 1989). In vivo, the linear form of the above equation is therefore more sensible:

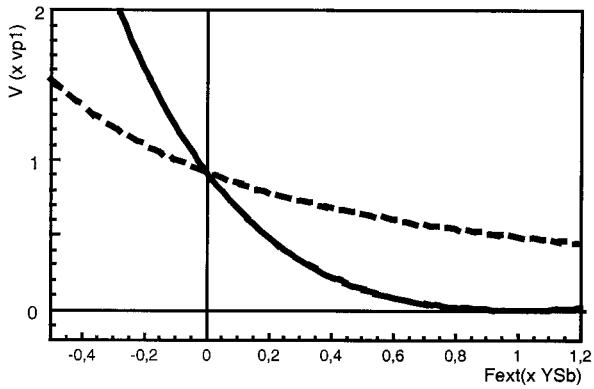

FIGURE 3 Force-velocity curve given by the one-dimensional model. The ratio of bacterium speed to polymerization speed is plotted versus the external force applied on the bacterium. – – –, Constant polymerization speed. ——, The polymerization speed depends on the stress normal to the bacterium surface.

$$\frac{v}{v_{p_l}} \simeq 1 - \frac{F_{\mathrm{ext}}}{Y \cdot S_b} \tag{6}$$

The polymerization speed varies with the stress

We shall now take into account the fact that the polymerization speed (v_p) at which the filaments are produced also depends on the applied forces. The external force F_{ext} induces at the molecular level a normal force f_{ext} on the growing filaments stuck between the bacterium surface and the cross-linked gel. If the filaments are compressed by the force f_{ext}, then the additional work required to add a monomer of size a is $\Delta W = f_{\mathrm{ext}} a$. Thermodynamics tells us that the effect of the force on both the off rate and the on rate of monomer addition at the tip of a growing filament can be described by introducing appropriate Boltzmann factors (Hill, 1987), such that the polymerization rate can be written as

$$v_p(f) = V_+ e^{-x(\Delta W/k_B T)} - V_- e^{(1-x)(\Delta W/k_B T)} \tag{7}$$

where $0 \leq x \leq 1$ is an adjustable parameter. Such a dependence has been demonstrated experimentally on microtubules by Dogterom and Yurke (1997), but their statistics were not sufficient to determine a value for x. We use Hill's thermodynamic description because it is generic and does not assume a precise mechanistic model of polymerization. It is not necessary to know x to determine the stall force f_s given for $v_p = 0$. Equation 7 gives $f_s = (k_B T/a)\ln$

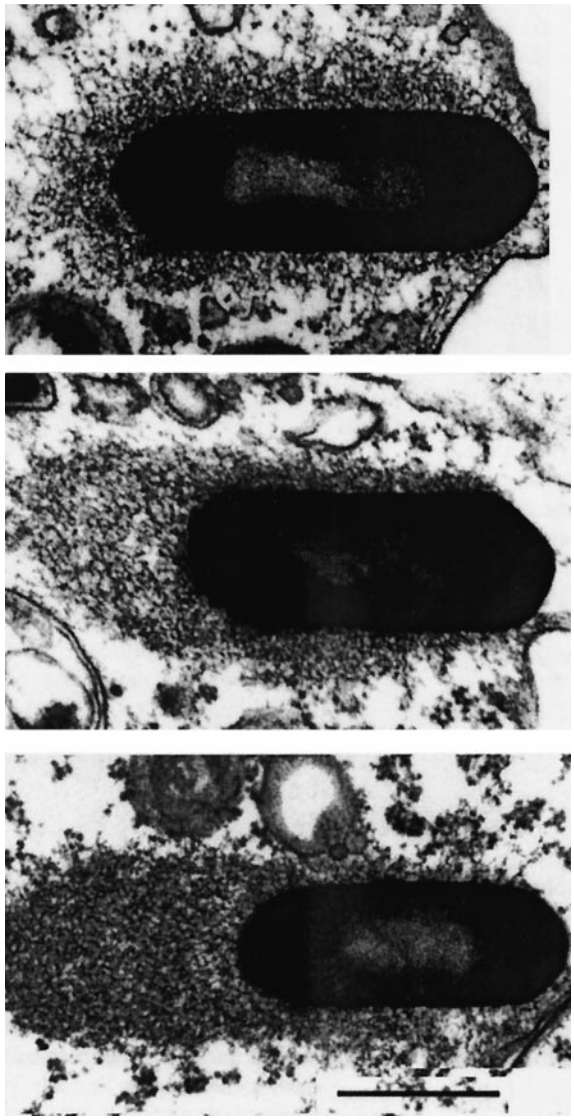

FIGURE 4 Thin sections of *Listeria monocytogenes* in infected cells inducing actin polymerization (courtesy Kocks et al., 1993). The bacterium is surrounded with actin, except at the front pole. The thickness of the gel over its cylindrical surface equals ~1/2 to 1 bacterium radius. Bar = 1 μm.

$(V_+/V_-) = (k_BT/a)\ln(\Delta G/k_BT)$, where $\Delta G = 14k_BT$ (Mogilner and Oster, 1996) is the free energy of the reaction of polymerization of one monomer. The stall force per filament should then be 1 pN. If we assume between 100 and 1000 filaments per *Listeria* tail section, the force required to stop the bacterium falls in the range of a nanoNewton, which is also the scale of the elastic forces in the problem. Thus the speed of the bacterium does not depend much on the external forces it encounters in vivo. It is determined by the polymerization rate and by the internal stresses exerted in the actin network.

In our equation, for the sake of simplicity, we will set $x = 1$, i.e., only the on rate is assumed to be affected by the stress. Thus, the polymerization speed is given by $v_{p_1} = v_{p_0}(1 - \epsilon_1)e^{-(\epsilon_1/\epsilon_0)}$ with the longitudinal strain $\epsilon_0 = k_BT/Yad^2$, where d is the mesh size of the gel. Assuming $d \approx 50$ nm, $\epsilon_0 \approx 1$.

Taking into account the variation of the polymerization speed, Eq. 6 becomes

$$\frac{v_p}{v_{p_0}} = \frac{1}{1 + F_{ext}/YS_b}\, e^{-(F_{ext}/\epsilon_0 YS_b)} \simeq 1 - 2\frac{F_{ext}}{YS_b} \qquad (8)$$

The slope of this new force-velocity curve (Fig. 3) is about twice the slope of the one obtained by assuming that the velocity is not stress dependent. This indicates that the variation of the polymerization speed affects the speed of the bacterium as much as the elastic compression of its tail. This concept will be required to understand the model of a bacterium pushed by a full tail (see Fig. 4).

The three-dimensional model

Bacterium pushed only by the external gel

Before considering the complete two-gel model, this section deals with a bacterium producing a gel only from the side, i.e., on the cylindrical surface. Although seemingly artificial, this model is based on observations of real systems. The bacterium *S. flexneri* uses the same trick as *Listeria monocytogenes* to propel itself forward: it produces an actin tail that appears to be hollow when observed by confocal microscopy (P. Cossart, personal communication). Moreover, Merrifield et al. (1999) showed that osmotic shock on a cell culture can induce endocytotic vesicles that move by forming an actin tail. This tail also appears to be hollow under a confocal microscope (personal communication).

We assume that actin is polymerized at the speed v_{p_2} normal to the cylindrically symmetrical surface of a bacterium. In addition, we assume that the filaments are immediately cross-linked and that no strain exists at first. As new material is continuously added at the bacterium surface, polymerization has to expand the older layer outward. One can view this model as a stack of rubber bands on a rigid cylinder, in which new bands are added from underneath, at the cylinder/rubber interface. If no symmetry breaking occurs, such a mechanism stops as the elastic energy increases and diverges like r^3, where r is the radius of the external layer. Such a cessation of growth has been demonstrated experimentally with spherical colloidal particles (Noireaux et al., 2000; Gerbal et al., 1999). Moreover, some *Listeria* do not produce a tail and are only surrounded by an actin sheath (Lasa et al., 1997). Alternatively, if the symmetry is broken, the radial energy built up around the bacterium relaxes in the tail. Between the bacterium and the tail, the gel changes its conformation to fulfill the new boundary conditions. It is not clear whether the symmetry breaking of the distribution of the gel around *Listeria* is spontaneous (as for Merrifield's vesicles) or is triggered by an external

factor such as the bacterium division, as shown in the case of the bacteria *S. flexneri* (Goldberg et al., 1994).

In the calculation below we describe the strain in the gel, using minimization of energy. Notations are shown in Fig. 5. On the cylindrical surface we assume the tangential speed of the gel v_0 to be constant. In the tail the gel speed becomes v. The gel grows continuously and reaches a maximum height r_m at the rear of the bacterium. Far away in the tail (assumed to be infinite), the gel thickness is $r_{out} - r_{in}$. Parameters α and 2δ are the dimensionless thicknesses of the gel above the bacterium and in the tail, respectively (see Table 1).

Calculation of strains and stresses in the gel: the stacked rubber band model

The expression of the radial stress in a stacked rubber band system produced at r_b and expanding to an outer radius r_{ext} is computed in Appendix I. At radius r the radial stress is

$$\sigma_{rr}(r; r_{ext}) = -\frac{1}{2} Y \frac{r_b}{r}\left[\left(\frac{r_{ext}}{r_b} - 1\right)^2 - \left(\frac{r}{r_b} - 1\right)^2\right] \quad (9)$$

This equation is valid for the gel above the bacterium and in the tail. In the tail, no solid surface restrains the inner radius. The radial component of the stress must vanish on the external and internal boundaries at $r = r_{in}$ and at $r = r_{out}$, respectively. The half-thickness δ of the gel in the tail is given by

$$\delta \triangleq \frac{r_{out}}{r_b} - 1 = 1 - \frac{r_{in}}{r_b} \quad (10)$$

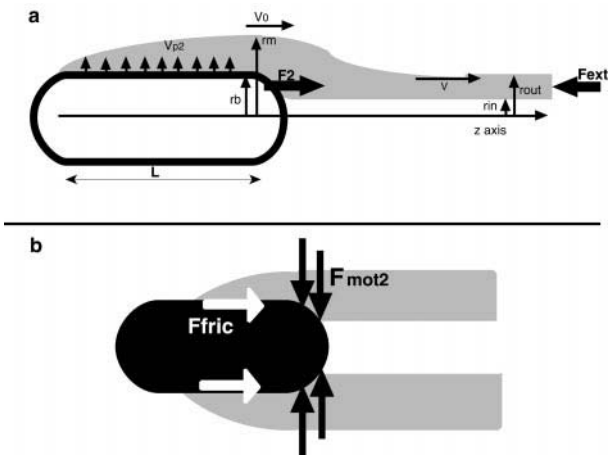

FIGURE 5 Notation for the 3D model, a bacterium producing only an external gel. (*a*) The gel is polymerized at speed v_{p_2} all over its cylindrical surface (with symmetry of revolution). In the reference frame of the bacterium, the gel moves at the speed v_0 and reaches the maximum external radius r_m over the bacterium. The tail is hollow and has inner and external radii r_{in} and r_{out}. It moves away from the bacterium at a speed v. (*b*) The force F_2 exerted by the external gel on the bacterium has two components: F_{fric}, due to the dynamic connection of the gel to the bacterium surface, and F_{mot_2}, due to the stress exerted by the gel on the back hemisphere.

The gel minimizes its elastic energy so that the axial stress in the tail must satisfy the equation (Landau and Lifchitz, 1967)

$$\sigma_z = \frac{\partial(E/\Delta V)}{\partial(\epsilon_{zz})} = -\frac{F_{ext}}{\pi(r_{out}^2 - r_{in}^2)} \quad (11)$$

where $E/\Delta V$ is the elastic energy per unit volume. Neglecting the nondiagonal terms like σ_{zr} (they must be of second order because they both vanish at the internal and external layers), the elastic energy has an axial and a radial contribution (see Appendix II):

$$\frac{E_{tail}}{\Delta V} = Y\left[\frac{(\epsilon_{zz})^2}{2} + \frac{1}{6}\delta^2\right] \quad (12)$$

We assume again here that the gel structure is homogeneous and that the Poisson ratio is 1/2. This is clearly a simplification, inasmuch as several works have shown that the filament orientation is not isotropic, although there is no clear consensus on this point (Sechi et al., 1997; Zhukarev et al., 1995). A small cylinder around the bacterium, despite the deformations, must have the same volume when it reaches the tail:

$$\pi(r_m^2 - r_b^2) = (1 + \epsilon_{zz})\pi(r_{out}^2 - r_{in}^2) \quad (13)$$

Using the dimensionless height of the gel $\alpha \triangleq (r_m - r_b)/r_b$, this equation becomes

$$\alpha(\alpha + 2) = (1 + \epsilon_{zz})4\delta \quad (14)$$

so that Eq. 12 can be written in term of ε_{zz} only:

$$\frac{E_{tail}}{\Delta V} = Y\left[\frac{(\varepsilon_{zz})^2}{2} + \frac{(\alpha(\alpha + 2))^2}{96}(1 + \epsilon_{zz})^{-2}\right] \quad (15)$$

As in the 1D model, another equation is provided by flux (Φ) conservation between the surface around the bacterium (of length L) and the section of the gel at the rear of the bacterium and through any section in the tail before depolymerization becomes important:

$$\Phi = L\pi r_b \cdot v_{p2} = S_b\alpha(\alpha + 2)v_0 = S_b 4\delta v \quad (16)$$

This gives a relation between the speeds and the gel thicknesses:

$$\frac{v}{v_0} = \frac{\alpha(\alpha + 2)}{4\delta} \quad (17)$$

The solution of Eq. 11 is then

$$\frac{v}{v_0} = 1 + \epsilon_{zz} = 1 - \frac{v}{v_0}\frac{F_{ext}}{\alpha(\alpha + 2)YS_b} + \frac{(\alpha(\alpha + 2))^2}{48}\left(\frac{v}{v_0}\right)^{-3} \quad (18)$$

Assuming that the speed of the gel does not change much from the bacterium to the tail ($v/v_0 \approx 1$), to the first order in

$v/v_0 - 1$ the expression becomes

$$\frac{v}{v_0} \approx 1 - \frac{F_{ext}}{\alpha(\alpha+2)Y \cdot S_b} + \frac{(\alpha(\alpha+2))^2}{48} \qquad (19)$$

For a thin gel above the bacterium ($\alpha < 1$), the expression is now $v/v_0 \approx 1 - F_{ext}/2\alpha Y \cdot S_b$, which is exactly equivalent to the expression found for the internal gel. Here the gel is produced at the back of the bacterium from a surface $2\alpha S_b$ (instead of S_b) at the speed v_0 (instead of v_{p_1}). The last term on the right-hand side of Eq. 19 shows that the strain is mainly radial when the gel is around the bacterium and becomes axial when it moves to the tail.

Force balance on the bacterium

We now must calculate the force exerted by the external gel on the bacterium. This is given by the integration of the stresses tangential and normal to the surface (Fig. 5 *b*):

$$F_2 = \int_{\text{bact. surface}} (\sigma_{nn} + \sigma_{nt})ds \qquad (20)$$

Let us first consider the normal term:

$$F_{mot_2} = \int_{\text{bact. surface}} \sigma_{nn} ds \qquad (21)$$

By symmetry of revolution, this expression vanishes when it is integrated over the cylindrical part. However, there is a nonvanishing contribution to the integral from the part of the back hemisphere where the gel is still in contact with the bacterium. The integration is carried out in Appendix III; the result is

$$F_{mot_2} = YS_b \frac{\alpha \cdot \delta}{3}(\alpha + \delta) \qquad (22)$$

For small deformations ($v \simeq v_0$) and α small, we have, from Eq. 16, $\alpha = 2\delta$, so we find a scaling law for the force:

$$F_{mot_2} \sim YS_b\alpha^3 \qquad (23)$$

This equation implies that the speed of the bacterium is no longer determined by the polymerization rate as in the 1D model. We call this force the "soap effect," because it recalls the rapid motion of a wet bar of soap slipping away as it is slowly squeezed by hand. If such a force seems unlikely at first sight, it is supported by the impressive motion of the mutant presented in the last part of this paper.

Let us now consider the tangential term of the stress. We show in Appendix V that for slow motion of the gel relative to the bacterium surface, the tangential force can be approximated by a friction law:

$$\int_{\text{bact. surface}} \sigma_{nt} ds \simeq F_{fric} = -\gamma v_0 \qquad (24)$$

The experimental observation that the bacterium is linked to the tail (Gerbal et al., 2000) shows that the friction coefficient is larger than a minimum value discussed in the following. We assume that each actin filament is coupled to the bacterium surface before it is released and moves to the tail with the gel. On a sufficiently long time scale during which many filaments attach to and detach from the bacterium surface, these transient links result in a friction force. Our experiments showed that the forces developed by an optical tweezer or by an electric field on the bacterium-tail connection were not sufficient to detach the bacterium from its tail. Thus, we were not able to measure γ experimentally. However, it is possible to put a lower bound on its value: assuming $v \approx v_0 \approx 0.2\ \mu m \cdot s^{-1}$, the force exerted by an electric field on the bacterium in our experiment was $\sim$1 pN applied over a typical time of 100 s. Observed by video microscopy, no separation between the tail and the bacterium (to accuracy 0.5 μm) was detected; therefore, $\gamma > 10^{-4}$ Pa · m · s. We can also propose an upper limit by requiring the consistency of our model: the bacterium can move forward if the motile force exceeds the friction: $F_2 = F_{mot_2} + F_{fric} > 0$, so that $\gamma < S_bY/v < 1$ Pa · m · s. The calculations presented below were performed for various values of γ in this range.

Also, as for the one-dimensional model, we suppose that the polymerization speed depends on the stress normal to the surface, so we have

$$v_{p_2} = v_{p_0} e^{-(\sigma_{rr} a d^2/k_B T)} \qquad (25)$$

Using the expression for the stress given by Eq. 9 and taking roughly the average value $r_m/2$ for the height of the gel over the bacterium surface, we have

$$v_{p_2} = v_{p_0} e^{-(\alpha/\alpha_0)^2} \qquad (26)$$

with $\alpha_0 \triangleq k_BT/Yad^2 \approx 1$.

The consistency of our model requires that we take into account the dependence of the polymerization speed on the stress: in the computation shown below, the axial strain remains lower than 0.1 in the tail (it is at maximum for γ = 1 Pa · m · s), so that the deformations are sufficiently small to be correctly treated by linear elasticity theory. This is not the case if the actin polymerization velocity is set constant in the computations leading to strains on the order of 1.

Force-velocity curves

The force-velocity curve is obtained when we solve for the speed in the force balance equation:

$$-F_{ext} = F_2 = F_{mot_2} + F_{fric} \qquad (27)$$

Details on the calculations are given in Appendix IV. Fig. 6 shows the numerical solutions for various values of γ.

These calculations demonstrate that increasing the internal friction (γ) or increasing the external force opposed to the motion have qualitatively the same effects: the bacterium slows down, the gel has time to grow thicker, and a larger stress builds up, which increases the driving force. The force-velocity curve of a bacterium driven by an external gel only is therefore also very stable, in agreement with the observed steady motion of *Shigella*. In the range of values of γ shown here, the computed gel thickness is in good agreement with the sizes observed in the electron micrographs provided by the literature. The remarkable difference with the 1D model is that the bacterium speed is no longer equal to the polymerization rate at zero external load: here v can be either greater than or less than v_{p_0}, depending on the value of γ. This is a consequence of the geometric change that the gel undergoes when moving from the vicinity of the bacterium to the tail, and of the nonlinearity introduced by the "soap effect." This raises the question of what happens in the complete system of a bacterium pushed by two gels that are cross-linked and leave the bacterium at the same speed.

The force-velocity curve for a bacterium pushed by both the external and the internal gel (Fig. 7 *a*) is given by the solution of the equation

$$F_{ext} = F_1 + F_2 = F_{mot_1} + F_{mot_2} + F_{fric} \qquad (28)$$

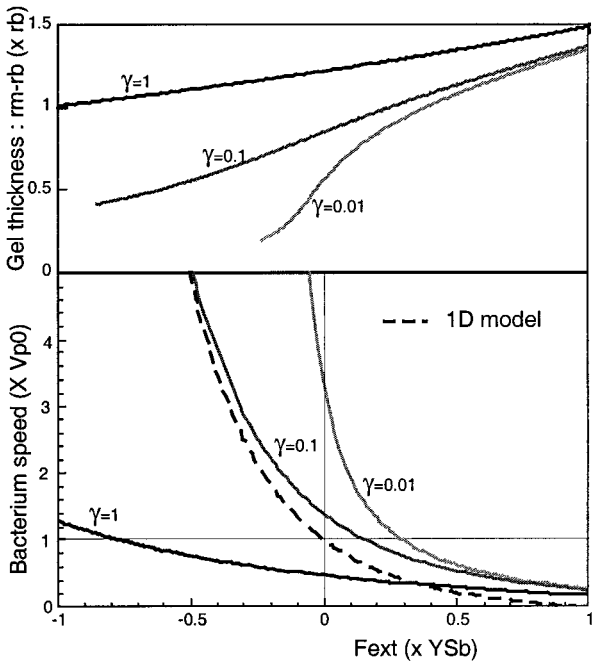

FIGURE 6 Velocity (*bottom*) and gel thickness α (*top*) of a bacterium pushed only by an external gel, as functions of the external force. The curves are plotted for various values of the friction parameter γ. Dashed line: force-velocity curve computed from the 1D model.

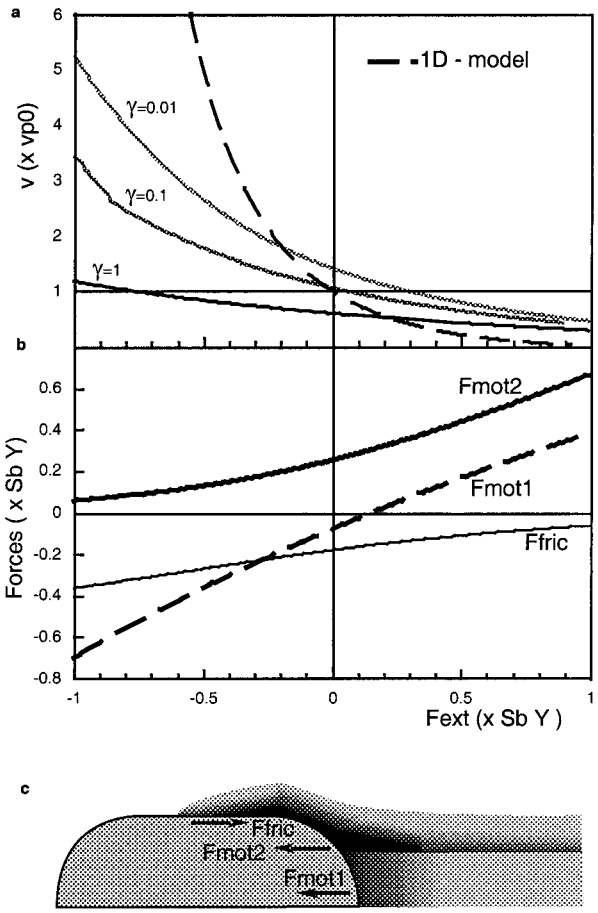

FIGURE 7 (*a*) Force-velocity curve for the two-gel model for various values of the friction parameter γ (*solid lines*). The dashed line is the curve obtained for the 1D model. (*b*) Force exerted by the various parts of the gel on the bacterium versus the external force F_{ext}. For a small external force, they exert antagonistic stresses on the bacterium (*c*) and cancel each other out.

In the presence of the two gels, the elastic force balances must remain the same: $F_1 = -\sigma_1 S_{t_1}$ and $F_2 = -\sigma_2 S_{t_2}$, but with the new condition $F_1 + F_2 = F_{ext}$. This implies the presence of shear strain in the tail: $\varepsilon_{rz} \neq 0$. Furthermore, a more realistic description requires the continuity of the radial stress σ_{rr} at the interface between the internal and external gels. Taking these conditions into account would have complicated the model without providing much insight into the mechanism, and so they are neglected for the sake of simplicity. Of course, we require that the two different parts of the gel have the same speed v. The complete set of equations used for the numerical calculations is presented in Appendix IV.

The results of the calculations are shown in Fig. 7, for various values of γ. Our model provides semiquantitative predictions and the order of magnitude of the forces involved in the motion. A more precise quantitative calculation would require us to take into account all of the terms of the stress tensors and the possibility of local plastic deformations.

The dependence of the polymerization rate on the normal stress solves the problem of the different velocity of the internal and external gels when considered independently: the linkage of the gel in the tail induces normal stresses on the bacterium surface that locally modulate the rate of actin polymerization. Removing the condition of the adaptive polymerization rate with the stress leads to huge nonrealistic strains in our calculations. This shows that it is not possible to change smoothly the configuration of a gel from a spherical to a linear geometry. The problem is solved if the gel growth speed is not constant along the surface. As a consequence, in the full model, the internal gel forces the bacterium velocity to be close to—although not equal to—the polymerization rate, when the external force is null.

The curve given by the full model is qualitatively similar to the one-dimensional curve, but it is even flatter: the velocity is even more constant when the motion of the bacterium is regulated by the two gels. As already predicted by the 1D model the amount of force required to slow down significantly the bacterium ($YS_b \approx 1$ nN) is much larger than the typical force it encounters in vivo (10–50 pN). This result is consistent with the observation of the very constant velocity of the wild-type *Listeria* and the fact that we were not able to induce any change in the velocity of the bacterium when exerting forces with optical tweezers or applying an electric field in the medium (in the range of 1–10 pN). The important new feature provided by the 3D model is that very strong antagonistic forces are applied on the bacterium by the different parts of the gel, as shown in Fig. 7, *b* and *c*. These forces almost compensate for each other, to provide the driving force opposing a weak external one. If the bacterium needs more force to propel itself forward, there is sufficient power in reserve: some parts of the gel become more compressed and increase the driving force. The amount of power available is not limiting; it is provided by the host cell through the hydrolysis of ATP caused by the actin polymerization reaction. The presence of these internal forces also shows that the gel holds the bacterium very tightly and that together they form a very robust system.

DYNAMIC DESCRIPTION OF THE LISTERIA MOTION

The hopping Listeria

The antagonistic forces predicted by the 3D model are a key concept in understanding the oscillatory motion of the *Listeria* mutant $ActA_{\Delta 21-97}$ (Lasa et al., 1997) described below.

To determine which subdomains of the ActA protein *Listeria* give the ability to induce the polymerization of actin, Lasa et al. performed genetic deletions of various parts of the *acta* gene (Lasa et al., 1995, 1997). By doing so, they isolated various types of *Listeria* mutants. Some cannot polymerize actin at all; others are still able to do so, but are stuck in an actin sheath and do not produce a tail. Most amazing is the mutant $ActA_{\Delta 21-97}$, which we named the "hopping *Listeria*," because it seems to move by jumps in a very discontinuous way, as shown in Fig. 8. The tail shows periodic spots of dense actin of ~ 2 μm in length (the size of a bacterium) spaced by distances varying from less than 1 to 4 μm. We have studied the motion of three of these hopping *Listeria*. The bacteria are stopped most of the time, and they achieve the greatest part of their displacement by bursts of speed that can be up to four times faster than the wild type (up to 1 $\mu m \cdot s^{-1}$). However, the average speed of the mutant is only 0.1 $\mu m \cdot s^{-1}$, about half the wild-type speed under the same conditions. At the beginning of a cycle, the bacterium is almost stopped. It is progressively surrounded by a fluorescent halo, showing clearly an accumulation of actin, and it seems to be stuck into a sheath. Meanwhile, the bacterium moves slowly until it starts to emerge from the sheath, at which point it accelerates very abruptly. The top speed is reached approximately when the bacterium fully emerges from the sheath (because the raw data are noisy, the top speed cannot be determined with an accuracy better than a few microns). Then the speed decreases down to zero and the mutant starts another cycle.

Several groups observed that wild-type *Listeria* may also have an oscillatory velocity when infecting some medium (Hela cell cytoplasm extract). Its tail also seems to be dashed. However, the speed variations are much less dramatic than for the mutant.

Most of the biological systems showing a highly nonlinear time dependence have found an explanation at the chemical level through enzymatic reaction (Goldbeter, 1996). Here we propose that the mechanism of the oscillations is physical rather than chemical, that they are due to the breaking of some connections between the bacterium and the gel as a consequence of the internal forces exerted at the bacterium surface predicted by the 3D model. A statistical model of the connection between the bacterium and the filaments is presented in Appendix V. There we demonstrate that the average connection time between the filaments and the surface depends on the "natural" chemical kinetics and on the force exerted by the tail. This force lowers the potential barrier that links the actin to the surface. Above a threshold, these links may break, thus inducing a dynamic instability.

The deletion of some peptides in the ActA protein may affect the enzymatic reaction in many different ways. It could change the energy potential and/or the kinetics of the links. One simple explanation is that if the turnover rate of the connections is slowed down, the mutant remains stuck within the new layer of polymerized actin. This would be in contrast with the wild type, which moves without breaking the transient links because their connection-release kinetics is faster. This means that the mutant has to store a larger amount of elastic energy to break the sheath. Slowing down the kinetics of the filament connections results, at a mesoscopic scale, in an increase in the effective friction parameter γ (see Appendix V). The force required to break a link

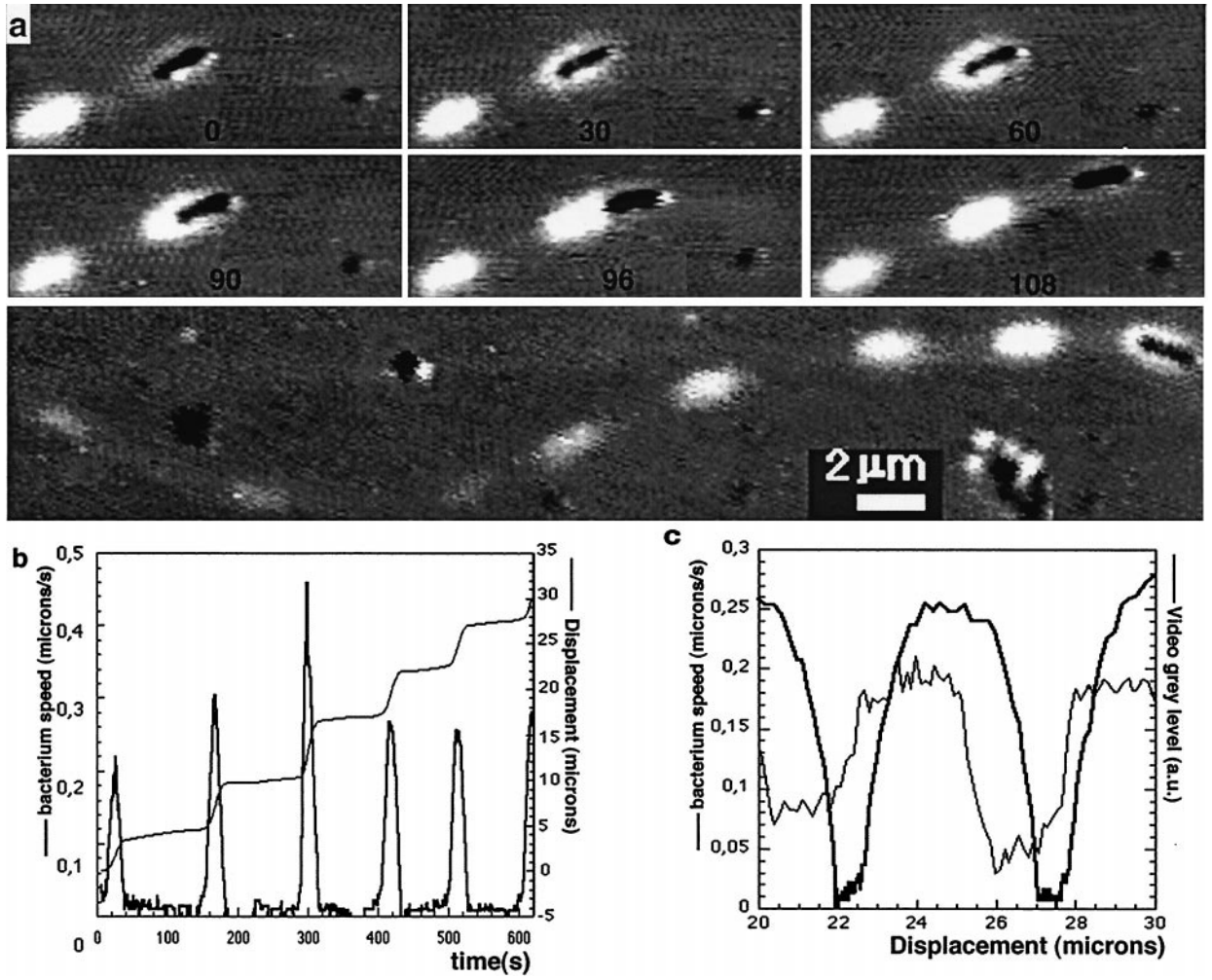

FIGURE 8 (*a*) Snapshots from a videotape of the mutant $ActA_{\Delta 21-97}$ (courtesy of P. Cossart et al.), seen at the same time by phase-contrast and fluorescent microscopy. The numbers indicate the time in seconds. (*b*) Kinematics record of the same mutant: Speed ($\mu m \cdot s^{-1}$) and curvilinear position (μm) as functions of time (s). The data shown have been filtered to suppress the high-frequency noise due to the uncertainty on the bacterium center in the video. (*c*) Speed and measurement of the video gray level intensity along the tail from the snapshots at time 108 s as a function of the position.

should be on the order of $\Delta G/a = 10k_BT/5$ nm $\approx$ 10 pN, where a is the size of an actin monomer and ΔG is a typical free energy associated with a coupling reaction ($14k_BT$ for actin polymerization). In Fig. 9, the amplitudes of the internal forces predicted by the 3D model are plotted as a function of γ. One can see that for very low values of γ, the internal tail is pulled by a force on the order of 200 pN ($YS_b \simeq 1$ nN). For large values of γ, forces that can reach 1 nN are exerted on the bacterium-external gel links. These forces are sufficient to break the linkage between the bacterium to the internal or the external gel if the numbers of active connections are 20 and 100 filaments, respectively.

The time-dependent equations

In this section the equations of the elastic model are modified slightly to account for the dynamics of the system. Calling $S(z, t)$ the cross-sectional area of the external gel at the position z, the flux conservation equation is

$$\frac{\partial S(z,t)}{\partial t} = 2\pi r_b v_{p_2} - \frac{\partial S(z,t)}{\partial z} v_0 \tag{29}$$

This can be simplified by assuming that the gel has a constant thickness β (dimensionless variable) above the cylindrical part (the gel cross section is $S_\beta = \pi r_b^2(\beta^2 - 1)$) before it reaches the thickness α above the back hemisphere (the surface area of which is $S_\alpha = \pi r_b^2(\alpha^2 - 1)$) (Fig. 10). The flux conservation equations are therefore

$$\frac{\partial S_\beta(t)}{\partial t} = \pi r_b v_{p_2}(\beta) - \frac{v_0}{L} S_\beta(t) \tag{30}$$

$$\frac{\partial S_\alpha(t)}{\partial t} = \frac{1}{r_b}(v_0 S_\beta(t) - v S_\alpha(t)) \tag{31}$$

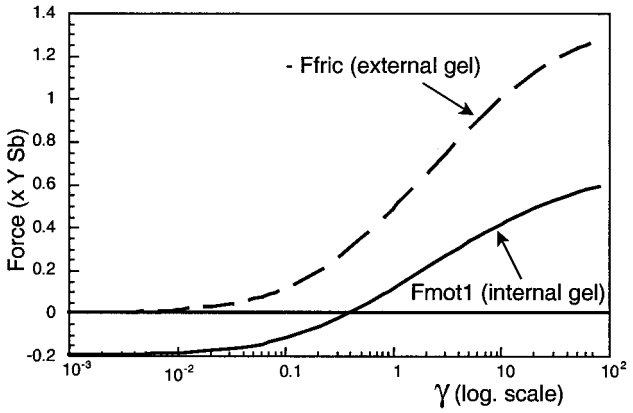

FIGURE 9 Diagram of the forces exerted by the internal gel (——) and the absolute value of the friction exerted by the external gel (– – –) on the bacterium as a function of the friction parameter γ (log scale).

where the polymerization speed v_{p_2} still depends on the normal stress: $v_{p_2}(\beta) = v_{p_0}e^{-\beta^2}$.

Another simplification can be used if we assume that the gel speed does not vary much when leaving the bacterium side: $v_0 \simeq v$. Notice that the steady-state solution is then simply

$$S_\beta = S_\alpha = \pi r_b L \frac{v_{p_2(\beta)}}{v} \tag{32}$$

We have not modified the flux equation for the internal gel; if it is compressed or extended, the gel returns to equilibrium on a length scale of a few mesh sizes. Thus, any hysteresis generated by a nonuniform strain in the internal gel would occur on a time scale too short to be relevant for the oscillations we want to describe.

The expressions of the forces pressing on the bacterium remain the same as in the steady-state description (Eqs. 8, 22, and 24), and the force balance is again

$$F_{mot_1}(t) + F_{mot_2}(t) + F_{fric}(t) = 0 \tag{33}$$

The time-dependent solutions were computed by simultaneously integrating the equations, using a fourth-order Runge-Kutta algorithm starting with the following initial condition: no gel is produced above the bacterium, and the initial speed is equal to the polymerization speed of the back gel, i.e., $S_\beta(t = 0) = S_\alpha(t = 0) = 0$ and $v(t = 0) = v_{p_0}$. Fig. 10 *b* shows the result of the computation when no ruptures have been introduced in the simulation. After an oscillatory period corresponding to the time required for the external gel to grow over the bacterium and to be located above the back hemisphere, the solution reaches the steady state already found in the time-independent equations. The type of solution remains the same whatever the value of γ; only the time scale changes. Indeed, it is possible to rewrite the set of

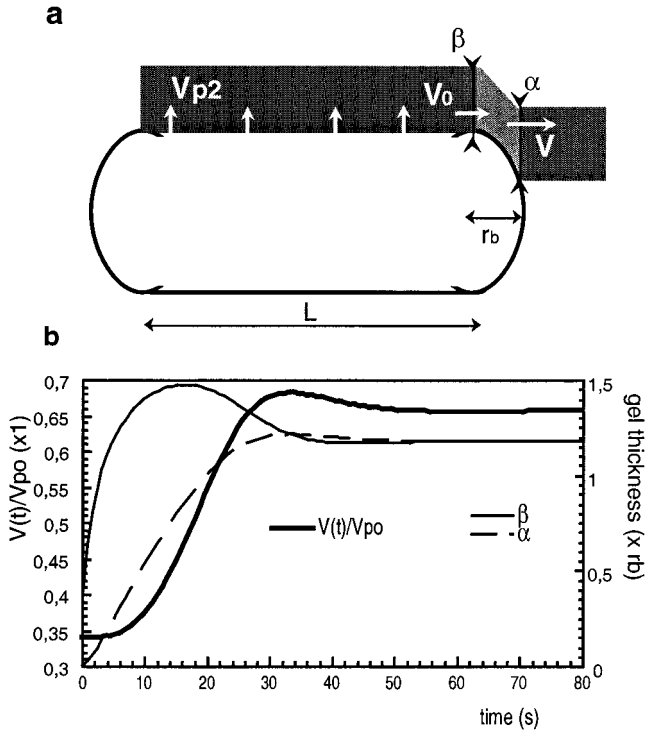

FIGURE 10 (*a*) Diagram of notation for the time-dependent flux conservation equation. Plot of the gel thickness β (over the cylindrical part) and α (over the back hemisphere). (*b*) Result of the numerical calculation, showing the transitory regime of the bacterium motion. α and β (*thin lines*) and the bacterium velocity (*thick line*) are plotted versus time for the case $\gamma = 0.1$.

equations as

$$v(t) = v_{p_1}\frac{1 + (1/4)\alpha^3(t)}{1 + \gamma v_{p_0}/YS_b} \tag{34}$$

$$\frac{\partial^2 S_\alpha(t)}{\partial t^2} + \left(\frac{v(t)}{r_b}\right)\left(1 + \frac{r_b}{L}\right)\frac{\partial S_\alpha(t)}{\partial t} + \frac{v^2}{r_b L}S_\alpha(t) = \pi v_{p_2} v(t) \tag{35}$$

and it is easy to show that they are stable. As expected, they are not sufficient to describe the "hopping *Listeria*" because they do not take into account a possible breakage of the links. A complete simulation of the rupture must contain the equations of Appendix V, particularly the Fokker-Planck equation 62, which controls the rate of connections between the gel and the surface. We have only used the quasistatic result giving the friction force as a function of the speed shown in Fig. 16. Qualitatively, this curve remains valid as long as no fast breakage occurs, i.e., before the friction law reaches its maximum. Once the threshold is reached, the links break catastrophically and a "stick-slip" transition occurs. This is modeled in our program by introducing a threshold force F_{s_2} above which the external gel is no longer connected and slips along the bacterium. Thus, the program contains the following conditions: if $|F_{fric}| > F_{s_2}$ then the

friction is arbitrarily lowered: $\gamma_{slip} = \gamma_{stick}/100$. Proportionally to the number of filaments (or the surface), a weaker force is sufficient to detach the internal gel from the bacterium: if $-F_{mot_1} > F_{s_1} = F_{s_1}/8$, then the gel 1 ruptures and no longer exerts a force: $F_{mot_1} = 0$.

The reconnection between the gels and the bacterium (γ returns to its initial value and F_{mot_1} equals its initial expression) occurs when one of these forces falls below its respective threshold.

The same Runge-Kutta algorithm was used to solve the equations completed by the breaking conditions. Fig. 11 shows the result in the case where $F_{s_1} = 0.1YS_b$ and $\gamma = 0.5$. These values are not fine-tuned because the above parameters may be chosen in a full domain of values and still produce qualitatively similar results. Comparison of Fig. 11 with the analysis of the mutant kinematics in Fig. 7 shows that our model is indeed able to reproduce the experimental data. Initially (Fig. 11), the same transitory period occurs as in the wild type described by the stable equations (Fig. 10 *b*). In the case of the mutant, it models the slow phase of a cycle. We found that the first condition required for the system to oscillate is that the initial friction (γ) is high enough with regard to the breakage thresholds. If this is the case, the bacterium moves slowly enough for the gel to accumulate (α increases steadily) and to strongly squeeze the bacterium on the back hemisphere. If the stress has time to reach the critical value of the yield force before the end of the transitory period, the linkage to the external gel breaks. A stick-slip transition occurs, the surface friction drops suddenly (we move from the right side to the left side of the diagram in Fig. 9), and the soap effect due to the accumulated gel pushes the bacterium forward. A second requirement for the oscillations is that the acceleration is high enough—the bacterium has to go faster than the polymerization rate—to also break the internal gel connections. Otherwise, another steady regime is reached in which the bacterium is simply pushed by the internal gel at about the polymerization rate, with the external gel loosely connected. But if the internal gel also detaches, the regime is unstable and we get oscillations: the bacterium is no longer retained by the internal gel and is propelled by the soap effect much faster than the polymerization rate. Consequently, not enough actin is polymerized to supply the diminishing gel on the side, so that its thickness (α and β) decreases. However, our calculations show that before the gel completely decays the bacterium has time to run in the fast regime over a distance comparable to several times its size. Once the gel thickness has vanished, the driving forces fall under their respective breaking thresholds and the filaments of the new layer are therefore connected again to the surface. The system has returned to its initial conditions and the mutant starts a new cycle. It can be surprising that when all of the links to both parts of the gel are broken, the bacterium does not free itself from its tail; although a stick-slip transition occurs, the external gel still surrounds the bacterium. The friction is reduced but is still much larger (typically $\gamma \simeq 10^{-3}$ Pa · m · s) than the friction due to the outer medium ($<10^{-6}$ Pa · m · s). Eventually, separation of the bacterium from its tail might occur. This is consistent with the observation of many simply diffusing bacteria coexisting in the medium with mutants pushed by a dashed tail.

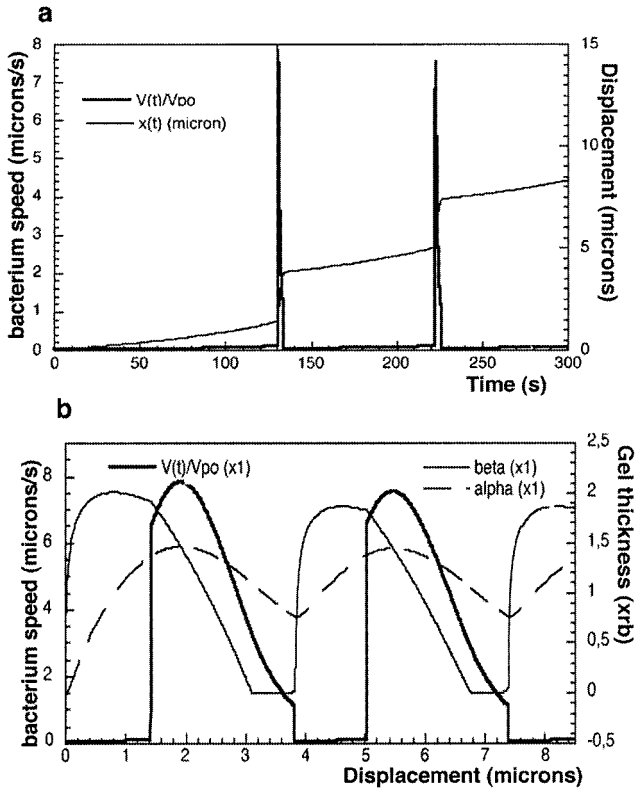

FIGURE 11 Result of the numerical calculation with a possible rupture of the gels. Here $\gamma = 0.5$ and $F_{s_1} = 0.1YS_b$. The velocity and the bacterium displacement are shown as a function of the time (*a*) and displacement (*b*). The gel thicknesses α and β around the bacterium are also plotted as function of the bacterium position.

Investigating other domains of values of F_{s_1} and γ leads to the simulation of other types of motion. For instance, for low values of γ, the internal gel can break; the filaments at the back are continuously pulled from the surface as they are connected to the external gel, which drives the bacterium faster than the polymerization speed. This is another steady regime in which the bacterium produces a "hollow tail"; the filament density is lower in the core than at the periphery of the tail. This simulation is consistent with the confocal observations of the tails of *S. flexneri* and of Merrifield's intracellular vesicles, which are indeed hollow.

CONCLUSION

Based on experimental results showing that *Listeria* are connected to their tail and using the measured value of the Young's modulus of the actin tail, we develop a theoretical

model of the propulsion of *Listeria*. The analysis is performed at a mesoscopic scale at which the actin tail gel is viewed as a continuous medium. The deformations are computed using the theory of linear elasticity. The purpose of this large-scale treatment is to consider the interaction between the many actin filaments involved. We show that some important characteristics of the motion arise from their collective behaviors.

We have described this complex system by a heuristic two-gel model to illustrate the main features of the propulsion mechanism. One result is that a smooth production of the tail is made possible because of the adaptive polymerization rate of actin at the surface of the bacterium, which depends on the local normal stress. Our model also shows that antagonistic forces are exerted on the bacterium by the gel with a magnitude much larger than the typical forces encountered by the bacterium when it moves through an infected cell. The tail behaves like a mechanical feedback system, keeping the speed of the bacterium fairly constant over a large range of force opposing its motion. This provides an explanation for the very steady motion of bacteria observed experimentally.

Our approach makes few assumptions about the microscopic mechanism at work in the polymerization/reticulation process; it can, in principle, be used with any microscopic mechanism, but it is a necessary step for describing the mesoscale physics of the propulsion. The mesoscopic level of analysis is absent in the Brownian ratchet model of Mogilner and Oster (1996). Their model describes a mechanistic description at the molecular level but is irrelevant for the mesoscopic behavior of the bacterium, because it does not consider the interactions between the filaments. The force-velocity curve characterizing the motion of the bacterium predicted by our study is qualitatively different from theirs, which exhibits a vanishing slope at zero external force. It is thus possible to discriminate between the two approaches by an experimental measure.

The design of an artificial *Listeria* system made of ActA protein-coated microspheres (Cameron et al., 1999; Noireaux et al., personal communication) will certainly be a useful system for testing several predictions of our model. For instance, by varying the shape of the beads and the area to which ActA is grafted, one could measure the strength of the "soap effect."

The antagonistic internal forces exerted on the bacteria surface predicted by our steady-state model lead to a simple understanding of the oscillatory motion of the mutant $ActA_{\Delta 21-97}$: at the microscopic level the mutation of the *acta* gene changes the connection kinetics of the links between the gel and the bacterium surface. It corresponds, at a physical or a mesoscopic level, to a modification of the surface properties, changing the polymerization rate and the effective friction between the gel and the bacterium. This can induce a stick-slip transition, resulting in the oscillatory motion of the mutant. Our model succeeds in reproducing the experimental data of its motion. It predicts that the strength of linkage between the mutant and the tail should be stronger during its slow phase and weaker during its rapid displacement. In micromanipulation experiments, this prediction could be tested by measurement of the force required to separate the *Listeria* from its tail for the wild type and the $ActA_{\Delta 21-97}$ mutant. Alternatively, an elegant way of probing the connection between the filaments and the bacterium surface would make use of the fluorescence resonant energy transfer technique. In the case of the mutant, one would directly obtain the bound and unbound times along the cycle.

An important consequence of our analysis is the possibility that the wild-type bacterium would show oscillations similar to those of the mutant, provided the biochemical conditions induce the required surface properties. Such a behavior has indeed been observed independently by the group of E. Friederich and J. Theriot.

It is natural to wonder if our analysis is applicable to describing the process of lamellipodium extension; in this case, the actin gel is inside the plasmic membrane and there is no reason for the "soap effect" to exist. However, although more complex, a corresponding level of mesoscopic description exists and deserves to be developed. Some aspects of our *Listeria* model might also apply in the case of the ameboid motion: a stick-slip transition could also be involved because of the competition between the pulling force on the cell body and the adhesion to the subtract (Heidenmann and Buxbaum, 1998).

Listeria is a typical system in which the effect of many proteins must be considered to explain the observations. Even a complete description of the biochemistry at the scale of a single protein is not sufficient to grasp the complexity of some biological phenomena, such as the oscillation we have analyzed. It is likely that biological systems take advantage of the complex physical processes emerging from the interaction between many identical molecules. This suggests that in many cases there is a further level of complexity to be explored once the molecular mechanisms are elucidated.

APPENDIX I: CALCULATION OF THE STRAINS AND STRESSES IN THE GEL: THE STACKED RUBBER BAND MODEL

Here we calculate the stress in a piece of cylindrical material of external radius r_{ext} (Fig. 12). Each layer has been extended from its relaxed state at radius r_b to the radius r. A freshly cross-linked layer at the bacterium surface is unstretched and has no azimuthal stresses: $\sigma_{\theta\theta}(r = r_b) = 0$.

In cylindrical coordinates, the elastic force balance $\nabla\sigma = 0$ becomes

$$\frac{d\sigma_{rr}}{dr} = \frac{\sigma_{\theta\theta} - \sigma_{rr}}{r} \tag{36}$$

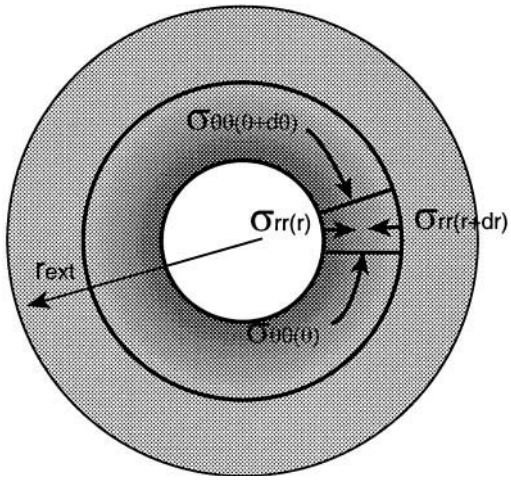

FIGURE 12 Schematic representation of the stress exerted in a cylindrical system made of elastic material.

which yields upon integration

$$\sigma_{rr}(r; r_{ext}) = \frac{1}{r}\int_{r_{ext}}^{r} dr' \sigma_{\theta\theta}(r') \tag{37}$$

In our problem, as the layer is pushed outward, its circumference increases and it induces an angular stress:

$$\sigma_{\theta\theta} = -Y\frac{r - r_b}{r_b} \tag{38}$$

The solution that gives a vanishing σ_{rr} at the external boundary of the gel is

$$\sigma_{rr}(r; r_{ext}) = -\frac{1}{2} Y \frac{r_b}{r}\left[\left(\frac{r_{ext}}{r_b} - 1\right)^2 - \left(\frac{r}{r_b} - 1\right)^2\right] \tag{39}$$

APPENDIX II: CALCULATION OF THE ELASTIC ENERGY IN THE TAIL

We now proceed to derive the elastic energy associated with the deformation of an elastic band of width $\Delta z'$ (in the tail), assuming that its width was Δz (at the end of the bacterium) (Fig. 13). The axial strain is $\epsilon_{zz} = \Delta z'/\Delta z - 1$. The inner and outer radius are given, respectively, by $r_{in} = r_b(1 - \delta)$ and $r_{out} = r_b(1 + \delta)$. For each layer, there is no azimuthal strain when its radius is r_b. The expressions for the normal and angular stresses are given by Eqs. 38 and 39. The elastic energy is given by

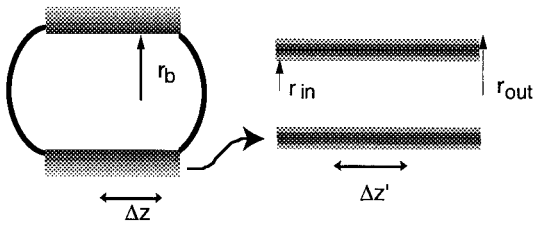

FIGURE 13 Notations for Appendix II. A cylindrical part of the gel of length Δz over the bacterium moves to the tail, where it extends to the length $\Delta z'$.

$$E_{tail} = \int_{\Delta V} u_{ij}\sigma_{ij} \tag{40}$$

where $\Delta V = \Delta Z' \pi(r_{out}^2 - r_{in}^2) = \Delta Z' \pi r_b^2 4\delta$. It is easy to calculate the axial contribution:

$$E_{extension} = \int_{\Delta V} u_{zz}\sigma_{zz} = \frac{1}{2} Y(\epsilon_{zz})^2 \Delta V \tag{41}$$

The radial contribution to the energy can be computed in two different ways. One is to integrate, using the expression given by Eq. 38:

$$E_{rad} = \int_{r_{in}}^{r_{out}} \sigma_{rr}(r = r_b; r'_{out}) 2\pi r_b \Delta z' \, dr'_{out} \tag{42}$$

This expression is the summation over the work paid for adding each layer at the radius r_{in} and extending the stack outward to the radius r'_{out}. Alternatively, it is simpler to sum over the work δW required to extend each layer from radius r_b up to radius r:

$$E_{rad} = \int_{r_{in}}^{r_{out}} \delta W = \frac{1}{2} Y 2\pi r_b \Delta z' \int_{r_{in}}^{r_{out}} \left(\frac{r}{r_b} - 1\right)^2 dr \tag{43}$$

Both methods give

$$E_{rad} = \frac{Y\pi r_b^2 \Delta z'}{3r_b^3}\left[(r_{out} - r_b)^3 - (r_{in} - r_b)^3\right] = \frac{2}{3} Y\pi r_b^2 \delta^3 \Delta z' \tag{44}$$

so that, considering only the diagonal terms in the stress matrix, the energy per volume unit in the tail is

$$\frac{E_{tail}}{\Delta V} = Y\left[\frac{(\varepsilon_{zz})^2}{2} + \frac{\delta^2}{6}\right] \tag{45}$$

APPENDIX III: FORCE EXERTED BY THE SIDE GEL ON THE BACTERIUM

The back hemisphere is modeled by a cone with a top angle θ. It bridges the cylindrical part of the bacterium (radius r_b) and the internal radius of the tail, $r_{in} = r_b(1 - \delta)$. Notations are given in Fig. 14. Before losing contact with the bacterium surface, the thickness of the gel is $r_m - r_b = \alpha r_b$. In the tail the thickness is $2\delta r_b$. The radius of the cone is expressed in terms of the abscissa z, so the radius of the gel touching the cone is $r_{int}(z) = r_b(1 - \delta z)$. The external radius of the gel over the cone is $r_{ext}(z) = r_b[1 + \alpha + (\delta - \alpha)z]$.

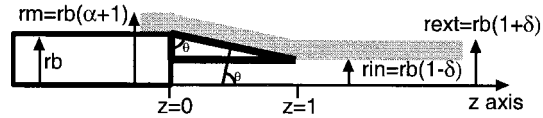

FIGURE 14 Notation for the calculation of the soap effect in Appendix III.

To obtain the expression of the force, one must integrate the equation

$$F_{\mathrm{mot}_2} = \int_{\text{bact. surface}} \sigma_{\mathrm{rr.}} \cos(\theta) \mathrm{d}s \tag{46}$$

Using the expression for $\sigma_{\mathrm{rr.}}$ given by Eq. 36, we have

$$F_{\mathrm{mot}_2} = YS_{\mathrm{b}} \frac{\alpha \cdot \delta}{3} (\alpha + \delta) \tag{47}$$

APPENDIX IV: EQUATIONS USED IN THE NUMERICAL COMPUTATION

The force balance is given by

$$F_{\mathrm{ext}} = F_{\mathrm{ext}_1} + F_{\mathrm{ext}_2} = F_{\mathrm{mot}_1} + F_{\mathrm{mot}_2} + F_{\mathrm{fric}} \tag{48}$$

with the previously established expressions of the forces (Eqs. 6, 22, and 24),

$$F_{\mathrm{mot}_1} = YS_{\mathrm{b}} \left(1 - \frac{v}{vp_1}\right)$$

$$F_{\mathrm{mot}_2} = YS_{\mathrm{b}} \frac{\alpha \cdot \delta(\alpha + \delta)}{3}$$

$$F_{\mathrm{fric}} = -\gamma v_0$$

F_{mot_1} is ignored when we consider a bacterium producing only the external gel.

The force balance equations are written as functions of the speeds:

$$\epsilon_1 = \frac{v}{v_{\mathrm{p}_1}} - 1 = -\frac{F_{\mathrm{ext1}}}{Y \cdot S_{\mathrm{t}_1}} = -\frac{F_{\mathrm{ext1}}}{Y \cdot S_{\mathrm{b}}} \frac{v}{v_{\mathrm{p}_1}} \tag{49}$$

$$\epsilon_2 = \frac{v}{v_0} - 1 = -\frac{F_{\mathrm{ext}_2}}{Y \cdot S_{\mathrm{b}}} \frac{v}{v_0} + \frac{(\alpha(\alpha + 2))^2}{48} \left(\frac{v}{v_0}\right)^{-3} \tag{50}$$

The flux conservation equations are

$$\pi r_{\mathrm{b}}^2 (\alpha(\alpha + 2)) v_0 = \pi r_{\mathrm{b}} L v_{\mathrm{p}_2} = \pi r_{\mathrm{b}}^2 4\delta \tag{51}$$

To take into account the dependence of the polymerization speed on the surface stress, we set

$$v_{\mathrm{p}2} = v_{\mathrm{p}0} e^{-(\alpha/\alpha_0)^2} \tag{52}$$

$$v_{\mathrm{p}1} = v_{\mathrm{p}0} e^{+(\epsilon_1/\epsilon_0)} = v_{\mathrm{p}0} e^{+(v/v_{\mathrm{p}_1} - 1)/\epsilon_0} \tag{53}$$

There are thus six equations and six unknowns: v, v_0, α, δ, F_{ext_1}, and F_{ext_2}, which we take in dimensionless forms:

$$w_1 = v/v_{\mathrm{p}1}, \quad w_2 = v/v_{\mathrm{p}2}, \quad d = \gamma v_{\mathrm{p}0}/YS_{\mathrm{b}},$$

$$\hat{F}_{\mathrm{ext}_2} = F_{\mathrm{ext}2}/YS_{\mathrm{b}}, \quad \hat{F}_{\mathrm{ext}_1} = F_{\mathrm{ext}1}/YS_{\mathrm{b}}, \quad \hat{F}_{\mathrm{ext}} = F_{\mathrm{ext}}/YS_{\mathrm{b}}$$

and the ratio between the two polymerization speed of the inner and outer gels: $r_{\mathrm{w}} = w_2/w_1 = vp_1/vp_2$.

These equations can be expressed as functions of the parameters r_{w}, α, w_2, and δ:

$$r_{\mathrm{w}} = \frac{v_{\mathrm{p}_1}}{v_{\mathrm{p}_0}} \frac{v_{\mathrm{p}_0}}{v_{\mathrm{p}_2}} = e^{(\epsilon_1/\epsilon_0)} e^{(\alpha/\alpha_0)^2} = e^{((w_2/r_w)-1)} e^{(\alpha/\alpha_0)^2} \tag{54}$$

$$\widehat{F_{\mathrm{ext}}} = r\left(1 - \frac{w_2}{r_{\mathrm{w}}}\right) + \frac{\alpha \cdot \delta(\alpha + \delta)}{3} - \frac{d}{(\alpha^2 - 1)} \frac{e^{((w_2/r_w)-1)}}{r_{\mathrm{w}}} \tag{55}$$

$$w_2 = \frac{l(1 + (\alpha(\alpha + 2))^2/48) + r \cdot r_{\mathrm{w}}}{\alpha(\alpha + 2) + \hat{F}_{\mathrm{ext}} + r} \tag{56}$$

$$\delta = \frac{l}{4w_2} \tag{57}$$

In case of a constant (strain independent) polymerization, we have $v_{\mathrm{p}_2} = v_{\mathrm{p}_1} = v_{\mathrm{p}_0}$, so $r_{\mathrm{w}} = 1$.

These equations are then numerically solved using an Euler algorithm.

APPENDIX V: STATISTICAL MODEL OF THE INTERACTION BETWEEN THE GEL AND THE BACTERIUM SURFACE

We present here a statistical model of the interaction between the gel and the bacterium surface. This model is generic in that it assumes the existence of a typical time τ, during which filaments are bound to the surface, and another typical time τ', during which they are unbound, but does not make any assumption about their respective values. The strong bacterium-tail cohesion found experimentally suggests that the bound time is not negligible compared to the unbound time.

In the following we calculate the tangential force exerted by the gel on the bacterium when it moves at a speed v_0 with respect to the bacterium. There are n sites on the surface from which filaments grow and are cross-linked to the gel (Fig. 15). The energy barrier preventing a filament from dissociating from a site is W_0. If the gel does not move ($v_0 = 0$), the enzymatic reaction sets a release rate ϖ_{c} at which the filaments detach "naturally" from the surface. If the gel moves ($v_0 \neq 0$), the filaments are pulled away from the enzymatic sites that are immobile, and the barrier potential W_0 is lowered. If the speed of the gel is fast compared to the turnover rate of the connections, the filaments are ripped off. If the gel has moved by a distance $x = v_0 t$, the filaments of the first layer are pulled, and each one bound to the enzymatic site experiences a force

$$F = cx = cv_0 t \tag{58}$$

in which c is an elastic modulus. For instance, if we assume the cross-links to be rigid, the pulling force F is due to the bending of the filaments, and $c = kTL_{\mathrm{p}}/l^3$, where L_{p} is the filament persistence length and l is the average distance between the enzymatic site and the nearest cross-link.

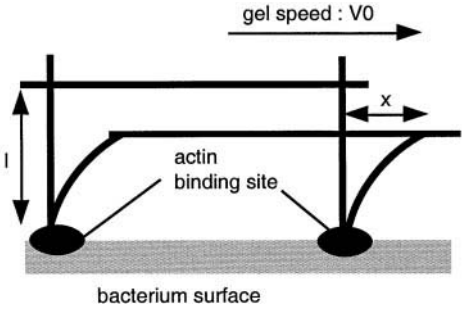

FIGURE 15 Schematic representation of the links between the gel and the bacterium surface. The gel moves at speed v_0, so the filament tips move a distance $x = v_0 t$. Assuming the cross-links are rigid, the filaments bend.

The force exerted on a typical scale of a monomer size a lowers the energy barrier, which becomes

$$W_b(t) = W_0 - Fa \tag{59}$$

The potential energy potential is thus lowered at the rate $\dot{W}$, defined by

$$\dot{W} = \dot{F}a = cv_0a \tag{60}$$

At a macroscopic scale, the total force exerted by the gel on the bacterium is the sum of all local forces F averaged over a cycle of attachment/detachment. So, calling n the total number of enzymatic sites and $P_c(t)$ the average probability that a filament is connected to it, the total tangential force exerted by the gel on the bacterium is

$$F_{fric} = nP_c(t)\langle F\rangle_{\tau+\tau'} \tag{61}$$

The number of connected sites at each time is ruled by a Fokker-Planck equation. $1/\tau$ is the frequency at which the nonconnected sites become cross-linked, and $1/\tau'$ is the frequency at which the connected sites are released. Thus,

$$\frac{dP_c(t)}{dt} = \frac{1 - P_c(t)}{\tau'} - \frac{P_c(t)}{\tau} \tag{62}$$

A correct calculation of the friction force involves solving this equation exactly. However, we can solve this problem in a quasistatic approximation, which is valid if the number of connected sites changes sufficiently slowly in time. So, in a mean-field picture, the steady-state solution is $P_c(t) = \tau/(\tau + \tau)$, and the macroscopic drag force on the bacterium is given by

$$F_{fric} = n\frac{\tau}{\tau + \tau'}\langle F\rangle_{\tau+\tau'} \propto n\frac{\tau}{\tau + \tau'}cv_0\tau \tag{63}$$

We must now estimate the average connection time τ between a site and the gel.

The probability that a site disconnects between time t and $t + dt$ ($t = 0$ when the filament is just linked to the gel) is the probability it has not broken until t times the probability it breaks during dt:

$$P(t)dt = \left(1 - \int P(t')dt'\right)\varpi_0 e^{-(W_b(t)/kT)}dt \tag{64}$$

Once integrated, this gives the probability

$$p(t) = P_0\exp\left(\frac{\dot{W}}{kT}t - \varpi_0 e^{-(W_b(t)/kT)}\frac{kT}{\dot{W}}(e^{\dot{W}t/kT} - 1)\right)$$

$$= P_0\exp\left(\varpi_b t - \frac{\varpi_c}{\varpi_b}(e^{\varpi_b t} - 1)\right) \tag{65}$$

where P_0 is the normalization factor, $\varpi_c = \varpi_0 e^{W_0/kT}$ is the chemical release rate, and $\varpi_b = \dot{W}/kT$ is the loading rate.

The average connection time τ is then given by $\tau = \int_0^\infty p(t)t\,dt$

Two limits can be investigated. If the speed of the gel is low ($v_0 \to 0$), ϖ_b vanishes, the release of the filaments is due to the chemical turnover. We then have $p(t)\overrightarrow{\varpi_b} \to 0\ P_0\exp(-\varpi_c t)$ and, simply, $\tau = 1/\varpi_c$. In the other limit, $\varpi_b > \varpi_c$, the filaments are ripped off essentially before they are pulled by the moving gel. The exponential in the exponential underscores the very fast breaking of the filaments, if the gel is displaced too far (Fig. 16 *a*). In such a case the distribution is sharp and is approximately centered around its average: $\tau = (1/\varpi_b)\ln(\varpi_b/\varpi_c)$, so that the connection time scales like $\tau \approx 1/\varpi_b \approx 1/\dot{W} \approx 1/v_0$, from Eq. 60.

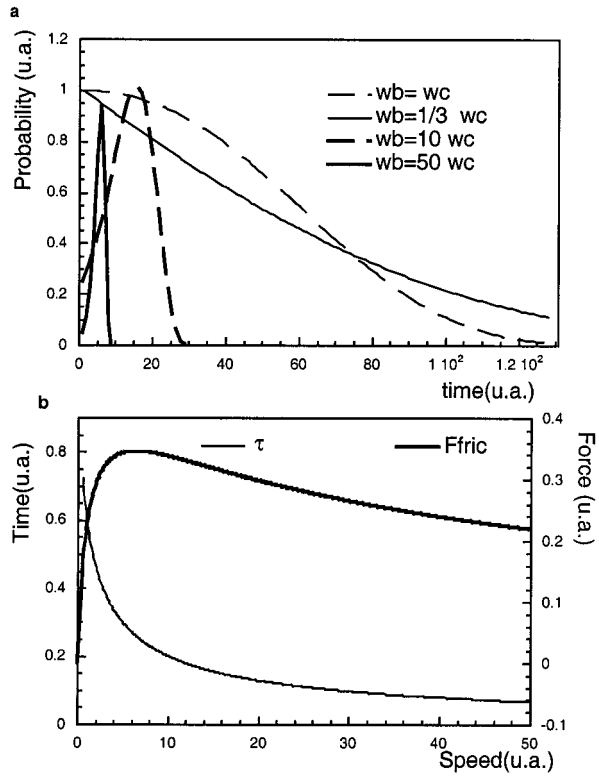

FIGURE 16 (*a*) Probability distribution of the time during which a site on the bacterium surface remains connected to the gel. The average of the distribution vanishes if ϖ_b goes over ϖ_c. Thick lines, $\varpi_b > \varpi_c$: thin lines, $\varpi_c > \varpi_b$. (*b*) Average connection time τ of a binding site to the gel versus the gel speed, and friction force (*thick line*). It decays after the filaments begin to rupture, thus weakening the gel-bacterium interaction.

F_{fric} plotted as a function of v_0 is shown in Fig. 16 *b*. It shows that at low speed $\tau = 1/\varpi_c$ is constant, and F_{fric} behaves like a classical friction force:

$$F_{fric} = \gamma v_0$$

with

$$\gamma = n\frac{\tau^2}{\tau + \tau'}c \tag{66}$$

In this case the microscopic cause of the friction is an elastic force that persists over a time τ. Averaged over a time longer than τ, this friction appears as a viscous force.

At the fastest speed, the breaking rate $\varpi_b \propto v_0$ dominates ϖ_c, some filaments start breaking, and the friction decreases: $F_{fric} \propto 1/v_0$. If the gel moves at a constant velocity, a steady state can be maintained. If it is the pulling force that is constant, this would lead to a catastrophic rupture of the connection between the gel and the bacterium, thus inducing a stick-slip transition at the gel/bacterium interface. In the case of *Listeria*, conditions are neither of constant velocity nor of constant force. In the breaking regime, our description breaks down (the steady-state solution of Eq. 62 is no longer valid), but its merit is to show the signature of the instability (the friction curve has a maximum). The transition corresponds to either a speed or a force threshold; the limit between the two regimes is approximately given by $\varpi_b = \varpi_c$. The speed threshold is $v_t = (kT/ac)\varpi_c$, which corresponds to a force threshold (or a yield force) of $F_t = n(\varpi_c^{-1}/\varpi_c^{-1} + \tau)(kT/a)$. Interestingly, if $\tau' \ll \varpi_c^{-1}$, the yield force does not depend on the turnover rate ϖ_c; in this limit, because most of the sites are connected to

the gel at any time, the force required to separate the gel from the bacterium depends essentially on their total number. On the contrary, the friction does depend on ϖ_c, which defines the time scale in which the elastic force is exerted. The conditions used in the computer simulations to model the stick-slip transition (see text) are consistent with the assumption that we are in this limit (supported by the strong tail-bacterium connection). The deletion of a part of the ActA protein can affect the bacterium surface properties (and thus the value of γ) by many means: for instance, by directly changing the binding energy (and therefore ϖ_b) or by modifying the kinetics of connection ϖ_c or simply the polymerization rate (it would also affect τ). This shows the interest of using a generic description of the system at a mesoscopic scale.

We thank Pascale Cossart, who kindly provided us with a video recording of the mutant *Listeria*. We also thank Marie-France Carlier, Dominique Pantaloni, and Frank Jülicher for their encouragement and their interest, which greatly contributed to this work. Nicolas Lartillot was great for his support and for cooking. Thanks to Stephanie Seveau for her everyday enthusiasm. Paul Chaikin and Yitzhak Rabin thank the Curie Institute for its hospitality during their stay in Paris, where this work was done.

REFERENCES

Alt, W., and M. Dembo. 1999. Cytoplasm dynamics and cell motion: two-phase flow models. *Math. Biosci.* 156:207–228.

Bray, D. 1992. Cell Movements. Garland Publishing, New York and London.

Bray, D., N. P. Money, M. Harold, and J. R. Bamburg. 1991. Response of growth cones to changes in osmolality of the surrounding medium. *J. Cell Sci.* 98:507–515.

Cameron, L. A., M. J. Footer, A. van Oudenaarden, and J. A. Theriot. 1999. Motility of ActA protein-coated microspheres driven by actin polymerization. *Proc. Natl. Acad. Sci. USA.* 96:4908–4913.

Clerc, P., and P. J. Sansonetti. 1987. Entry of Shigella flexneri into HeLa cells: evidence for directed phagocytosis involving actin polymerization and myosin accumulation. *Infect. Immun.* 55:2681–2688.

Cossart, P., and C. Kocks. 1994. The actin-based motility of the facultative intracellular pathogen *Listeria monocytogenes. Mol. Microbiol.* 13: 395–402.

Cudmore, S., P. Cossart, G. Griffiths, and M. Way. 1995. Actin-based motility of vaccinia virus. *Nature.* 378:636–638.

Dabiri, G. A., J. M. Sanger, D. A. Portnoy, and F. S. Southwick. 1990. *Listeria monocytogenes* moves rapidly through the host-cell cytoplasm by inducing directional actin assembly. *Proc. Natl. Acad. Sci. USA.* 87:6068–6072.

Dogterom, M., and B. Yurke. 1997. Measurement of the force-velocity relation for growing microtubules. *Science.* 278:856–860.

Evans, E. 1993. New physical concepts for cell amoeboid motion. *Biophys. J.* 64:1306–1322.

Evans, E., and A. Yeung. 1989. Apparent viscosity and cortical tension of blood granulocytes determined by micropipet aspiration. *Biophys. J.* 56:151–160.

Gerbal, F., V. Laurent, A. Ott, M. Carlier, P. Chaikin, and J. Prost. 2000. Measurement of the elasticity of the actin tail of *Listeria monocytogenes. Eur. Biophys. J.* 29:134–140.

Gerbal, F., V. Noireaux, C. Sykes, F. Julicher, P. Chaikin, A. Ott, J. Prost, R. Goltsteyn, E. Friederich, D. Louvard, V. Laurent, and M. Carlier. 1999. On the "Listeria" propulsion mechanism. *Pramana J. Phys.* 53:155–170.

Goldberg, M., and J. A. Theriot. 1995. *Shigella flexneri* surface protein IcsA is sufficient to direct actin based motility. *Proc. Natl. Acad. Sci. USA.* 92:6572–6576.

Goldberg, M., J. A. Theriot, and P. J. Sansonetti. 1994. Regulation of surface presentation of IcsA, a *Shigella* protein essential to intracellular movement and spread, is growth phase dependent. *Infect. Immun.* 62:5664–5668.

Goldbeter, A. 1996. Biochemical Oscillations and Cellular Rhythms. Cambridge University Press, Cambridge.

Heidenmann, S. R., and R. E. Buxbaum. 1998. Cell crawling: first the motor, now the transmission. *J. Cell Biol.* 141:1–4.

Hill, T. L. 1987. Linear Aggregation Theory in Cell Biology. Springer-Verlag, New York.

Kocks, C., E. Gouin, M. Tabouret, P. Berche, H. Ohayon, and P. Cossart. 1992. *L. monocytogenes*-induced actin assembly requires the actA gene product, a surface protein. *Cell.* 68:521–531.

Kocks, C., R. Hellio, P. Gounon, H. Ohayon, and P. Cossart. 1993. Polarized distribution of *Listeria monocytogenes* surface protein ActA at the site of directional actin assembly. *J. Cell Sci.* 105:699–710.

Landau, L., and E. Lifchitz. 1967. Théorie de l'élasticité. Mir, Moscow.

Lasa, I., V. David, E. Gouin, J. B. Marchand, and P. Cossart. 1995. The amino-terminal part of ActA is critical for the actin-based motility of *Listeria monocytogenes*; the central proline-rich region acts as a stimulator. *Mol. Microbiol.* 18:425–436.

Lasa, I., E. Gouin, M. Goethals, K. Vancompernolle, V. David, J. Vandekerckhove, and P. Cossart. 1997. Identification of two regions in the N-terminal domain of ActA involved in the actin comet tail formation by *Listeria monocytogenes. EMBO J.* 16:1531–1540.

Loisel, T., R. Boujemaa, D. Pantaloni, and M. Carlier. 1999. Reconstitution of actin-based motility of *Listeria* and *Shigella* using pure proteins. *Nature.* 401:613–616.

Marchand, J. B., P. Moreau, A. Paoletti, P. Cossart, M. F. Carlier, and D. Pantaloni. 1995. Actin-based movement of *Listeria monocytogenes*: actin assembly results from the local maintenance of uncapped filament barbed ends at the bacterium surface. *J. Cell Biol.* 130:331–343.

Merrifield, C. J., S. E. Moss, C. Ballestrem, B. A. Imhof, G. Griese, I. Wunderlich, and W. Almen. 1999. Endocytic vesicles move at the tips of actin tails in cultured mast cells. *Nat. Cell. Biol.* 1:72–74.

Mitchison, T. J., and L. P. Cramer. 1996. Actin-based cell motility and cell locomotion. *Cell.* 84:371–379.

Mogilner, A., and G. Oster. 1996. Cell motility driven by actin polymerization. *Biophys. J.* 71:3030–3045.

Mogilner, A., and G. Oster. 1999. The polymerization ratchet model explains the force-velocity relation for growing microtubules. *Eur. Biophys. J.* 28:235–242.

Mounier, J., A. Rytr, M. Coquis-Rondon, and P. Sansonetti. 1990. Intracellular and cell-to-cell spread of *Listeria monocytogenes* involves interaction with F-actin in the enterocytelike cell. *Infect. Immun.* 58: 1048–1058.

Noireaux, V., R. M. Golsteyn, E. Friederich, J. Prost, C. Antony, D. Louvard, and C. Sykes. 2000. Growing an actin gel on spherical surfaces. *Biophys. J.* 78:1643–1654.

Sechi, A. S., J. Wehland, and J. V. Small. 1997. The isolated comet tail pseudopodium of *Listeria monocytogenes*: a tail of two actin filament populations, long and axial and short and random. *J. Cell Biol.* 137: 155–167.

Smith, G. A., D. A. Portnoy, and J. A. Theriot. 1995. Asymmetric distribution of the *Listeria monocytogenes* ActA protein is required and sufficient to direct actin-based motility. *Mol. Microbiol.* 17:945–951.

Southwick, F., and D. Purich. 1998. *Listeria* and *Shigella* actin-based motility in host cells. *Trans. Am. Clin. Climatol. Assoc.* 109:160–172.

Theriot, J. A., T. J. Mitchison, L. G. Tilney, and D. A. Portnoy. 1992. The rate of actin-based motility of intracellular *Listeria monocytogenes* equals the rate of actin polymerization. *Nature.* 357:257–260.

Tilney, L. G., and D. A. Portnoy. 1989. Actin filaments and the growth, movement and spread of the intracellular bacterial parasite, *Listeria monocytogenes. J. Biol. Chem.* 109:1597–1608.

Wang, Y. L. 1985. Exchange of actin subunits at the leading edge of living fibroblasts: possible role of treadmilling. *J. Cell Biol.* 101:597–602.

Welch, M. D., A. Iwamatsu, and T. J. Mitchison. 1997. Actin polymerization is induced by Arp2/3 protein complex at the surface of *Listeria monocytogenes. Nature.* 385:265–269.

Welch, M., J. Rosenblatt, J. Skoble, D. Portnoy, and T. Mitchison. 1998. Interaction of human Arp2/3 complex and the *Listeria monocytogenes* ActA protein in actin filament nucleation. *Science.* 281:105–108.

Zhukarev, V., F. Ashton, J. Sanger, and H. Shuman. 1995. Organization and structure of actin filament bundles in *Listeria*-infected cells. *Cell Motil. Cytoskeleton.* 30:229–246.